Soft-Tissue Lesions: When Can We Exclude Sarcoma?

Avneesh Chhabra[1]
Theodoros Soldatos

OBJECTIVE. A wide spectrum of space-occupying soft-tissue lesions may be discovered on MRI studies, either as incidental findings or as palpable or symptomatic masses. Characterization of a lesion as benign or indeterminate is the most important step toward optimal treatment and avoidance of unnecessary biopsy or surgical intervention.

CONCLUSION. The systemic MRI interpretation approach presented in this article enables the identification of cases in which sarcoma can be excluded.

Space-occupying soft-tissue lesions are frequently detected on MRI studies, either as incidental findings or during the evaluation of palpable abnormalities or focal symptoms. In this setting, the exclusion of malignancy is the initial and most important step of the treatment algorithm. Histologic examination remains the definite means to establish the diagnosis, but routine biopsy of all soft-tissue lesions is not practical or cost effective. Although more than 99% of soft-tissue lesions are benign, those referred for MRI evaluation have a higher likelihood of being malignant because they have raised some concern on the part of the physician. However, a considerable number of lesions among them still have a pathognomonic appearance on MRI, rendering their biopsy redundant. It is therefore important that benign lesions are excluded using MRI, before embarking on invasive procedures. In addition, a number of patients cannot undergo surgical or interventional procedures and may suffer from unnecessary morbidity and mortality [1–4]. This article provides a systematic approach to the assessment of soft-tissue mass lesions, along with a guide to the stepwise evaluation and prudent use of various pathognomonic imaging features that assist in differentiating benign from indeterminate, and thus potentially malignant, entities.

Imaging Technique

Accurate assessment of the location, extent, borders, and signal intensity is paramount for the characterization of soft-tissue lesions. A typical imaging protocol for potential tumor evaluation includes multiplanar conventional T1-weighted fat-suppressed fluid-sensitive (fat-suppressed T2-weighted, T2-weighted, or STIR) and unenhanced and contrast-enhanced fat-suppressed T1-weighted sequences [1]. In cases of inhomogeneous fat suppression, the quality of the images can be improved with subtraction technique. A T2*-weighted (gradient-echo) sequence may added in cases of suspected pigmented villonodular synovitis and calcific tendinitis to assess for blooming artifact related to hemosiderin deposition and hydroxyapatite deposition disease (HADD), respectively [5]. The unenhanced and contrast-enhanced images must be obtained with identical imaging parameters to allow adequate and quantitative assessment of enhancement. The contrast-enhanced fat-suppressed T1-weighted images should be compared with caution to the non–fat-suppressed unenhanced T1-weighted images, because some masses, such as ganglion cysts and adventitial bursitis, appear hyperintense on fat-suppressed T1-weighted images, simply because fat suppression has been applied, and this imaging effect could be inadvertently mistaken for contrast enhancement [1] (Fig. 1). If possible, IV contrast imaging should be performed with a dynamic time-resolved technique. The temporal resolution of the latter sequence can be used to assess the hemodynamics of lesions and to obtain an MR angiogram, which can assist in determining their vascular status for preoperative planning [6]. Chemical-shift imaging may also be further be added to the imaging protocol to examine possible associated marrow abnormalities.

Keywords: MRI, sarcoma, soft-tissue tumors

DOI:10.2214/AJR.12.8719

Received February 11, 2012; accepted after revision April 18, 2012.

[1]Both authors: Russell H. Morgan Department of Radiology and Radiological Science, Johns Hopkins Hospital, 601 N Caroline St, Baltimore, MD 21287. Address correspondence to A. Chhabra (achhabr6@jhmi.edu).

AJR 2012; 199:1345–1357

0361–803X/12/1996–1345

TABLE 1: Stepwise Evaluation of Soft-Tissue Masses

Points to Consider Regarding the Lesion in Question	Entities to Consider and Exclude[a]
Could it be a normal structure?	Accessory, supernumerary, or anomalous muscle; muscle strain; muscle hernia; and unencapsulated fat tissue
Does it have fluid?	Hematoma, seroma, ganglion cyst or myxoma, intramuscular cyst, geyser phenomenon, Morel-Lavallée lesion, and abscess
Does it have fat?	Lipoma, hemangioma, elastofibroma, heterotopic ossification, and neural fibrolipomatous hypertrophy
Does it have prominent areas of T2 hypointensity?	Fibroma, fibromatosis, soft-tissue callus, and hydroxyapatite deposition disease
Is it located within or adjacent to a joint?	Synovial chondromatosis, pigmented villonodular synovitis, ganglion cyst or geyser phenomenon, loose body, synovial hemangioma, lipoma arborescens, and particle disease
Is it related to a tendon or ligament?	Giant cell tumor, hydroxyapatite deposition disease, amyloid, gout, and xanthoma
Is it a predominantly vascular abnormality?	Venous malformation, arteriovenous malformation, and lymphatic malformation
Is it a nerve-related abnormality?	Peripheral nerve sheath tumor, fibrolipomatous hamartoma, and perineurioma

[a]These are entities that should be considered and excluded according to MRI findings, before reporting a soft-tissue mass as indeterminate and, thus, potentially malignant.

Imaging Assessment

The reader should carefully evaluate the lesion in terms of its size, borders, and internal signal characteristics on all imaging sequences. MRI features of soft-tissue lesions that are suggestive of malignancy include ill-defined borders; infiltration or invasion of adjacent structures; size greater than 5 cm; deep location; heterogeneous T1 and T2 signal intensity; high T2 signal intensity of surrounding tissues, indicative of edema disproportionate to the size of the lesion, a feature not applicable in patients with previous surgery, radiation, or suspected inflammation; necrosis; intralesional hemorrhage; bone or neurovascular involvement; early contrast enhancement, followed by plateau or washout; and peripheral, nodular, or heterogeneous internal enhancement [4–7]. The prevalence of these features is, however, variable [4, 7, 8]. In addition, a considerable number of benign lesions show many of the aforementioned features. The reader should therefore follow the following systematic stepwise approach to define lesions as benign or indeterminate (i.e., potentially malignant or sarcoma).

Stepwise Evaluation

The following outline of a series of evaluation steps (summarized in Table 1) should be followed for optimal soft-tissue lesion assessment.

Step 1: Could the Lesion Be a Normal Structure?

Care should be taken to avoid misdiagnosing normal anatomic variations as tumors. Although most parts of the body are symmetric, discrepancy in size, course, or orientation between the sides may lead to the subjective impression of the presence of a mass lesion [2]. A wide array of accessory, supernumerary, and anomalous skeletal muscles have been described in the literature and are detected as a space-occupying mass causing palpable lesion, compression syndrome, or incidental findings on imaging studies (Fig. 2). The aforementioned muscles should not cause a diagnostic dilemma because they feature signal and enhancement characteristics similar to the adjacent muscles on all pulse sequence and attach to bones via tendinous insertions [3, 9]. Muscle strains are associated with intramuscular edema or fluid collections, which can be extensive and inhomogeneous, mimicking an infiltrative process. Strained muscles, however, maintain their striated architecture and show gradual resolution of findings on short-term follow-up studies (Fig. 3). Intramuscular hematoma produces peripheral enhancement, as opposed to solid intramuscular mass lesion [10, 11]. Muscle hernias are associated with epimysial defects, which allow muscles to bulge into the subcutaneous fat, and present as soft-tissue masses on clinical and imaging examination. The entity typically presents in the lower extremities and is diagnosed based on the detection of the fascial defect and the visualization of anatomic continuity and similarity in signal intensity, architecture, and enhancement characteristics between the protruded lesion and the underlying muscle [12, 13]. Ultrasound is usually preferred for real-time assessment of these lesions. Localized prominent unencapsulated fat tissue, usually resulting from rapid changes in weight or steroid use, may also mimic a neoplastic process. The typical fat signal characteristics and absence of contrast enhancement enables accurate characterization [2].

Step 2: Does the Lesion Contain Mostly Fluid?

Soft-tissue hematomas frequently manifest as space-occupying lesions, mimicking neoplasms in patients with or without a clear history of trauma. In most cases, history and clinical findings are exculpatory; however, MRI may be used to evaluate indeterminate lesions or underlying tumors. Although hematomas may feature variable signal characteristics, areas of T1 hyperintensity corresponding to methemoglobin, a peripheral rim of hemosiderin in subacute to chronic stages of the lesion, surrounding soft-tissue edema, and an absence of contrast enhancement or a thin rim of peripheral enhancement strongly support the diagnosis, and lesions may simply be followed to resolution [8, 14, 15] (Fig. 4).

Seromas, ganglion cysts, and intramuscular cysts (such as in the setting of rotator cuff tear) typically show low and high signal intensity on T1-weighted and T2-weighted images, respectively, and again enhance only peripherally after contrast agent administration [16, 17] (Fig. 5). Geyser phenomenon refers to a large synovial cyst that arises from the acromioclavicular joint and projects into the subcutaneous tissues and is typically associated with a long-standing full-thickness rotator cuff tear and acromioclavicular ligament tears [18, 19] (Fig. 6). In Morel-Lavallée (or degloving) lesions, a posttraumatic space-occupying cavity is formed in the layers of the subcutaneous tissues, between the skin and deep fascia, which fills with blood, lymph, debris, or fat. Apart from a history of recent or remote trauma, these lesions are well defined and are oval, fusiform, or crescent-shaped on MRI and may show fluid-fluid levels, septations, and variable signal intensity, but they have no or only peripheral contrast enhancement [20, 21] (Fig. 7). Soft-tissue abscesses usually arise

in the setting of local inflammation (cellulitis) and present on MRI as organized fluid collections with surrounding edema or inflammatory changes, cutaneous ulcer, or sinus tracts and early enhancing wall, which becomes more intense over time [22, 23].

In myxoid tumors, either benign (myxoma) or malignant (e.g., myxoid liposarcoma, myxofibrosarcoma, and myxoid pleomorphic sarcoma), the myxoid component commonly produces a fluidlike T2 hyperintense signal. The lesions may erroneously be perceived as simple cysts, unless streaks of fat or solid components (present in many myxoid liposarcomas) are recognized or if contrast agent is administered to show lacy or patchy enhancement (present in benign myxoid lesions) [24, 25] (Fig. 8).

Step 3: Does the Lesion Contain Fat?

A mass is considered as containing fat when it features T1 areas of T1 hyperintensity that are suppressed on fat-saturated images. Masses composed entirely of fat, with only minimal thin septations and without nonfatty nodular components, can safely be diagnosed on MRI as simple lipomas [26, 27]. The latter are commonly encountered in the subcutaneous tissues and feature signal characteristics identical to the subcutaneous fat on all sequences. Heterotopic lipomas can develop within skeletal muscles, tendon sheaths, joints, and nerves. Intramuscular lesions may look heterogeneous; on careful evaluation, however, the apparent septations are related to spared or traversing muscle fibers around the fat lobules of the lesions, featuring signal and enhancing characteristics similar to those of the remainder of the muscle or the adjacent normal muscles [7, 28] (Fig. 9). Lesions with thicker septations or "dirty-fat" appearance, attributed to fat necrosis, fibrosis, inflammation, or myxoid change, are described as atypical lipomatous tumors and are histologically similarly classified as well-differentiated liposarcomas, which more commonly develop in the deeper tissues, such as the retroperitoneum, and show slow growth. Depending on the local institutional treatment strategy and underlying patient functional status, the aforementioned lesions may be biopsied or followed for interval growth [29]. Lesions that are larger than 10 cm, contain septa thicker than 2 mm, have nodular nonfatty components, and show significant interval growth are suspicious for liposarcomas and warrant biopsy [1]. Other benign lesions that may contain macroscopic fat include hemangioma, elastofibroma, heterotopic ossification, and neural fibrolipomatous hypertrophy. Elastofibromas are most commonly seen along the inferomedial border of the scapula beneath the latissimus dorsi muscle and feature fibrofatty striations. They are highly vascular lesions, and biopsy should be avoided, given their typical location and MRI appearance [7, 30] (Fig. 10). Heterotopic ossification may look aggressive on MRI, especially if there is no history of injury, and the findings are analyzed in isolation. Radiograph or CT may show a peripheral mature rim of calcification and progressive central calcification on follow-up imaging [31].

Step 4: Does the Lesion Feature Prominent Areas of T2 Hypointensity?

The detection of areas of T2 hypointensity (with respect to the signal intensity of the skeletal muscles) can narrow the differential diagnosis, predominantly to entities that contain fibrous tissue, hemosiderin, or calcification [1]. Possible lesions include fibroma and fibromatosis (common in the plantar and palmar fascia), callous, HADD, giant cell tumor of the tendon sheath, gout, and amyloid. Plantar fibroma is typically seen as a pea-shaped mass in relation to the central cord of the plantar fascia in the midfoot. Apart from T2 hypointensity, it shows homogeneous enhancement after contrast agent administration [32] (Fig. 11). Plantar fibromatosis (Ledderhose disease) is seen as a locally aggressive lesion with sheetlike thickenings and multifocal masses that feature mixed T2 signal intensity, depending on cellularity and the percentage of fibrous tissue. Heterogeneous enhancement is typical [33, 34]. Soft-tissue callus is a superficial soft-tissue thickening that develops as a response to chronic mechanical pressure. It is usually found in the submetatarsal soft tissues of the forefoot and features intermediate-to-low signal intensity on MRI, along with poor enhancement [35] (Fig. 12). HADD usually develops at the supraspinatus tendon insertion as a T2-hypointense deposit, which blooms on T2*-weighted images. Radiograph correlation is helpful to detect calcifications. When the inflammation is extensive, the entity may mimic a mass lesion and might mislead unwary readers [36, 37] (Fig. 13). MRI shows the extent of the inflammation, as well as the associated rotator cuff tears.

Step 5: Is the Lesion Located Within or Adjacent to a Joint?

It is exceedingly rare for the malignant lesions to begin in a joint [38]; therefore, malignancy can be essentially excluded on the detection of an intraarticular mass. In cases of intraarticular masses, the differential diagnosis should include synovial chondromatosis, pigmented villonodular synovitis, ganglion cyst, loose bodies, synovial hemangioma, and lipoma arborescens. In synovial chondromatosis, the synovial lesions may coalesce to form a nonenhancing conglomerate mass, which is usually isointense and hyperintense to muscle on T1- and T2-weighted images, respectively. In advanced stages, the individual lesions may be identified within the mass, featuring central signal intensity analogous to fatty bone marrow and low-signal periphery analogous to cortical bone [39, 40]. Pigmented villonodular synovitis is characterized by hypertrophied synovium that presents as a focal masslike lesion or as diffuse areas of synovial thickening with low signal lining on T2- or T2*-weighted images (Fig. 14). There may be associated bone erosions [41, 42]. Ganglion cyst, which is usually associated with previous injury, is located adjacent to the joint capsule, meniscus, labrum, and specific congenital bursa or adventitial bursa and features T2-hyperintense and nonenhancing or peripherally enhancing uni- or multilocular contents. A neck can usually be traced from the lesion to the originating fluid-containing structure. Loose bodies, which can be large and often contain marrow and hypointense peripheral lining, do not enhance and are more conspicuous on T2*-weighted images (Fig. 15). The contents may be heterogeneous (e.g., due to posttraumatic hemorrhage, infectious exudate, rheumatoid rice bodies, or chondromatosis nodules). Synovial hemangioma appears as a lobulated mass with intermediate and markedly high signal intensity on T1- and T2-weighted images, respectively, and usually features low–signal-intensity linear structures corresponding to fibrous septa or vascular channels [40, 43, 44]. In lipoma arborescens, frondlike projections of hypertrophied synovium show signal intensity similar to that of fat on all imaging sequences [45–47]. It is very common to see the appearances of partial or complete lipoma arborescens as part of synovial fibrofatty hypertrophy in internally deranged joints, especially surprapatellar pouch of the knee joint, rather than as a primary process. The latter case may, however, require synovectomy. Despite its name, synovial sarcoma only rarely occurs within joints. In cases of previous arthroplasty, prosthesis, or graft, low–signal-intensity debris, capsular thickening, joint effusion, and synovitis may mimic an aggressive process but are suggestive of particle disease (Fig. 16).

Step 6: Is the Lesion Related to a Tendon or Ligament?

For lesions that are attached to tendon or ligaments, a wide spectrum of benign entities should be excluded before considering the possibility of a sarcoma. The focal form of pigmented villonodular synovitis may arise in tendon sheaths, in which case it is termed "giant cell tumor of the tendon sheath" and typically appears as a space-occupying lesion of low signal intensity on all pulse sequences, with variable degrees of contrast enhancement [48, 49]. HADD most commonly affects the rotator cuff insertion, and the acute phase of the disease is associated with marrow and soft-tissue edema that can mimic a neoplasm [50]; however, the characteristic round deposits of low signal intensity on all imaging sequences (particularly in T2*-weighted images) are sufficient to establish the diagnosis (Fig. 13). Xanthomas (localized accumulations of lipid in the setting of hypercholesterolemia or hyperlipoproteinemia) may involve tendons (most commonly the Achilles tendon) and cause focal fusiform tendon enlargement, mimicking a neoplasm. Affected tendons feature speckled or reticulated architecture and heterogeneous signal intensity on all imaging sequences, an appearance that is more obvious on fat-suppressed T1-weighted images [51] (Fig. 17). Amyloid and gout deposition may occur in tendons, causing focal masslike enlargement that is hypointense on T2-weighted images. The lesions are usually periarticular, whereas the underlying history of chronic systemic disease and hyperuricemia points to the prospective diagnosis [52, 53] (Fig. 18).

Step 7: Is It a Predominantly Vascular Lesion?

Intense enhancement, dilated vessels within or adjacent to the lesion in question, flow voids, and round signal voids should suggest the presence of a vascular mass [54]. Vascular malformations may cross fascial boundaries and involve multiple different tissues; however, they typically show no perilesional edema or mass effect and are serpiginous in nature. Hemangioma shows a homogeneously enhancing soft-tissue mass and is seen in children as congenital capillary or cavernous form. It may be further characterized as noninvoluting congenital hemangioma or rapidly involuting hemangioma, but virtually all are seen in soft tissues before 10 years of age. Venous malfornations are more commonly seen in young and adult patients and these appear as heterogeneous lobulated masses that show moderate and high signal intensity on T1- and T2-weighted images, respectively (Fig. 19). These lesions commonly feature a central angiomatous core of T2 hyperintensity, as well as fat proliferation along the circumference of the vascular complex. Small internal round flow voids correspond to phleboliths. Intralesional flow voids indicate a high-flow vascular lesion, typically an arteriovenous malformation. The flow voids represent dysplastic vessels in the center of the lesion and are usually associated with dilated tortuous feeding arteries and draining veins. The absence of flow voids is indicative of slow-flow variants, such as venous or lymphatic malformations [55–58]. Lymphatic malformations are typically seen in the setting of Klippel-Trenaunay-Weber syndrome and show peripheral enhancement only. Intralesional blood-fluid levels may coexist [59]. Time-resolved contrast imaging is useful in differentiating the aforementioned malformations and depicting arteriovenous areas, which appear as early venous drainage during the arterial phase of the examination.

Step 8: Could the Lesion Be Nerve Related?

Space-occupying lesions located along the anatomic course of peripheral nerves are suspicious for peripheral nerve sheath tumors. The diagnosis is strongly suspected on the presence of one or more of characteristic imaging signs, such as the tail, target, split-fat, fascicular, and bag-of-worms signs. Accurate differentiation between benign and malignant tumors is not reliably possible by MRI, although malignancy is strongly suggested in cases of ill-defined or infiltrative lesions [60]. In our recent experience, diffusion imaging, particularly diffusion tensor imaging, is a useful adjunct tool short of biopsy to differentiate benign from malignant lesions. Higher apparent diffusion coefficient values indicating less cellularity are seen in benign lesions and tractography differences exist among benign and malignant lesions [61]. Focal fusiform nerve enlargement associated with fatty proliferation and thickening of nerve bundles is indicative of fibrolipomatous hamartoma [61, 62]. The latter is associated with mononeuropathy and, potentially, macrodystrophia lipomatosa. Fibrolipomatous hamartoma features a classic coaxial cable appearance on axial images and a spaghetti appearance on longitudinal images (Fig. 20). Perineurioma is another benign tumor that can be prospectively diagnosed on MRI. Diagnostic criteria include young age, insidious motor functional loss, fusiform nerve enlargement outside the entrapment sites, uniform honeycomblike fascicular enlargement, homogeneous enhancement, and lack of history of neurocutaneous syndromes, such as neurofibromatosis or schwannomatosis [63] (Fig. 21).

Conclusion

The implementation of a systematic approach in the MRI evaluation of soft-tissue lesions assists in the accurate identification of benign entities and the proper selection of indeterminate (and potentially malignant) cases, thereby limiting the number of unwarranted biopsies and surgical interventions.

References

1. Wu JS, Hochman MG. Soft-tissue tumors and tumorlike lesions: a systematic imaging approach. *Radiology* 2009; 253:297–316
2. Kim SY, Park JS, Ryu KN, Jin W, Park SY. Various tumor-mimicking lesions in the musculoskeletal system: causes and diagnostic approach. *Korean J Radiol* 2011; 12:220–231
3. Sookur PA, Naraghi AM, Bleakney RR, Jalan R, Chan O, White LM. Accessory muscles: anatomy, symptoms, and radiologic evaluation. *RadioGraphics* 2008; 28:481–499
4. Gielen JL, De Schepper AM, Vanhoenacker F, et al. Accuracy of MRI in characterization of soft tissue tumors and tumor-like lesions: a prospective study in 548 patients. *Eur Radiol* 2004; 14:2320–2330
5. Kransdorf MJ, Murphey MD. Radiologic evaluation of soft-tissue masses: a current perspective. *AJR* 2000; 175:575–587
6. van Rijswijk CS, Geirnaerdt MJ, Hogendoorn PC, et al. Soft-tissue tumors: value of static and dynamic gadopentetate dimeglumine-enhanced MR imaging in prediction of malignancy. *Radiology* 2004; 233:493–502
7. Lin EC. Malignant versus benign soft tissue lesions. In: Lin EC, Escott EJ, Garg KD, Bleicher AG, Alexander D, eds. *Practical differential diagnosis for CT and MRI.* New York, NY: Thieme, 2008:268 –269
8. Stacy GS, Kapur A. Mimics of bone and soft tissue neoplasms. *Radiol Clin North Am* 2011; 49:1261–1286, vii
9. Cheung Y, Rosenberg ZS. MR imaging of the accessory muscles around the ankle. *Magn Reson Imaging Clin N Am* 2001; 9:465–473, x
10. Yoshioka H, Anno I, Niitsu M, Takahashi H, Matsumoto K, Itai Y. MRI of muscle strain injuries. *J Comput Assist Tomogr* 1994; 18:454–460
11. Boutin RD, Fritz RC, Steinbach LS. Imaging of sports-related muscle injuries. *Radiol Clin North Am* 2002; 40:333–362, vii
12. Mellado JM, Perez del Palomar L. Muscle hernias of the lower leg: MRI findings. *Skeletal Radiol* 1999; 28:465–469
13. Egan TJ, Lemos M, Iorio R. Muscular herniation of the lower extremities. *Am J Orthop* 1998; 27:102–106
14. Unger EC, Glazer HS, Lee JK, Ling D. MRI of

extracranial hematomas: preliminary observations. *AJR* 1986; 146:403–407

15. Taïeb S, Penel N, Vanseymortier L, Ceugnart L. Soft tissue sarcomas or intramuscular haematomas? *Eur J Radiol* 2009; 72:44–49
16. Beaman FD, Peterson JJ. MR imaging of cysts, ganglia, and bursae about the knee. *Radiol Clin North Am* 2007; 45:969–982, vi
17. Steiner E, Steinbach LS, Schnarkowski P, Tirman PF, Genant HK. Ganglia and cysts around joints. *Radiol Clin North Am* 1996; 34:395–425, xi–xii
18. Chalian M, Soldatos T, Faridian-Aragh N, et al. MR evaluation of synovial injury in shoulder trauma. *Emerg Radiol* 2011; 18:395–402
19. Cooper HJ, Milillo R, Klein DA, DiFelice GS. The MRI geyser sign: acromioclavicular joint cysts in the setting of a chronic rotator cuff tear. *Am J Orthop* 2011; 40:E118–E121
20. Kalaci A, Karazincir S, Yanat AN. Long-standing Morel-Lavallée lesion of the thigh simulating a neoplasm. *Clin Imaging* 2007; 31:287–291
21. Mellado JM, Perez del Palomar L, Diaz L, Ramos A, Sauri A. Long-standing Morel-Lavallée lesions of the trochanteric region and proximal thigh: MRI features in five patients. *AJR* 2004; 182:1289–1294
22. Beaman FD, Kransdorf MJ, Andrews TR, Murphey MD, Arcara LK, Keeling JH. Superficial soft-tissue masses: analysis, diagnosis, and differential considerations. *RadioGraphics* 2007; 27:509–523
23. Harish S, Chiavaras MM, Kotnis N, Rebello R. MR imaging of skeletal soft tissue infection: utility of diffusion-weighted imaging in detecting abscess formation. *Skeletal Radiol* 2011; 40:285–294
24. Peterson KK, Renfrew DL, Feddersen RM, Buckwalter JA, el-Khoury GY. Magnetic resonance imaging of myxoid containing tumors. *Skeletal Radiol* 1991; 20:245–250
25. Sundaram M, Baran G, Merenda G, McDonald DJ. Myxoid liposarcoma: magnetic resonance imaging appearances with clinical and histological correlation. *Skeletal Radiol* 1990; 19:359–362
26. Kransdorf MJ, Bancroft LW, Peterson JJ, Murphey MD, Foster WC, Temple HT. Imaging of fatty tumors: distinction of lipoma and well-differentiated liposarcoma. *Radiology* 2002; 224:99–104
27. Kransdorf MJ, Moser RP Jr, Meis JM, Meyer CA. Fat-containing soft-tissue masses of the extremities. *RadioGraphics* 1991; 11:81–106
28. Matsumoto K, Hukuda S, Ishizawa M, Chano T, Okabe H. MRI findings in intramuscular lipomas. *Skeletal Radiol* 1999; 28:145–152
29. Gaskin CM, Helms CA. Lipomas, lipoma variants, and well-differentiated liposarcomas (atypical lipomas): results of MRI evaluations of 126 consecutive fatty masses. *AJR* 2004; 182:733–739
30. Yu JS, Weis LD, Vaughan LM, Resnick D. MRI of elastofibroma dorsi. *J Comput Assist Tomogr* 1995; 19:601–603
31. Ochsner JE, Sewall SA, Brooks GN, Agni R. Best cases from the AFIP: elastofibroma dorsi. *RadioGraphics* 2006; 26:1873–1876
32. McNally EG, Shetty S. Plantar fascia: imaging diagnosis and guided treatment. *Semin Musculoskelet Radiol* 2010; 14:334–343
33. Narváez JA, Narváez J, Ortega R, Aguilera C, Sánchez A, Andía E. Painful heel: MR imaging findings. *RadioGraphics* 2000; 20:333–352
34. Robbin MR, Murphey MD, Temple HT, Kransdorf MJ, Choi JJ. Imaging of musculoskeletal fibromatosis. *RadioGraphics* 2001; 21:585–600
35. Bancroft LW, Peterson JJ, Kransdorf MJ. Imaging of soft tissue lesions of the foot and ankle. *Radiol Clin North Am* 2008; 46:1093–1103, vii
36. Garcia GM, McCord GC, Kumar R. Hydroxyapatite crystal deposition disease. *Semin Musculoskelet Radiol* 2003; 7:187–193
37. Siegal DS, Wu JS, Newman JS, Del Cura JL, Hochman MG. Calcific tendinitis: a pictorial review. *Can Assoc Radiol J* 2009; 60:263–272
38. Helms CA, Major NM, Anderson MW, Kaplan PA, Dussault R. Arthritis and cartilage. In: Helms CA, Major NM, Anderson MW, Kaplan PA, Dussault R, eds. *Musculoskeletal MRI*. Philadelphia, PA: Saunders, 2009:111–122
39. Milgram JW. Synovial osteochondromatosis: a histopathological study of thirty cases. *J Bone Joint Surg Am* 1977; 59:792–801
40. Sheldon PJ, Forrester DM, Learch TJ. Imaging of intraarticular masses. *RadioGraphics* 2005; 25:105–119
41. Garner HW, Ortiguera CJ, Nakhleh RE. Pigmented villonodular synovitis. *RadioGraphics* 2008; 28:1519–1523
42. Hughes TH, Sartoris DJ, Schweitzer ME, Resnick DL. Pigmented villonodular synovitis: MRI characteristics. *Skeletal Radiol* 1995; 24:7–12
43. Greenspan A, Azouz EM, Matthews J 2nd, Decarie JC. Synovial hemangioma: imaging features in eight histologically proven cases, review of the literature, and differential diagnosis. *Skeletal Radiol* 1995; 24:583–590
44. Llauger J, Monill JM, Palmer J, Clotet M. Synovial hemangioma of the knee: MRI findings in two cases. *Skeletal Radiol* 1995; 24:579–581
45. Adelani MA, Wupperman RM, Holt GE. Benign synovial disorders. *J Am Acad Orthop Surg* 2008; 16:268–275
46. Vilanova JC, Barcelo J, Villalon M, Aldoma J, Delgado E, Zapater I. MR imaging of lipoma arborescens and the associated lesions. *Skeletal Radiol* 2003; 32:504–509
47. Ryu KN, Jaovisidha S, Schweitzer M, Motta AO, Resnick D. MR imaging of lipoma arborescens of the knee joint. *AJR* 1996; 167:1229–1232
48. Jelinek JS, Kransdorf MJ, Shmookler BM, Aboulafia AA, Malawer MM. Giant cell tumor of the tendon sheath: MR findings in nine cases. *AJR* 1994; 162:919–922
49. De Beuckeleer L, De Schepper A, De Belder F, et al. Magnetic resonance imaging of localized giant cell tumour of the tendon sheath (MRI of localized GCTTS). *Eur Radiol* 1997; 7:198–201
50. Yang I, Hayes CW, Biermann JS. Calcific tendinitis of the gluteus medius tendon with bone marrow edema mimicking metastatic disease. *Skeletal Radiol* 2002; 31:359–361
51. Bude RO, Adler RS, Bassett DR. Diagnosis of Achilles tendon xanthoma in patients with heterozygous familial hypercholesterolemia: MR vs sonography. *AJR* 1994; 162:913–917
52. Cobby MJ, Adler RS, Swartz R, Martel W. Dialysis-related amyloid arthropathy: MR findings in four patients. *AJR* 1991; 157:1023–1027
53. McQueen FM, Doyle A, Dalbeth N. Imaging in gout: what can we learn from MRI, CT, DECT and US? *Arthritis Res Ther* 2011; 13:246
54. Olsen KI, Stacy GS, Montag A. Soft-tissue cavernous hemangioma. *RadioGraphics* 2004; 24:849–854
55. Fayad LM, Hazirolan T, Bluemke D, Mitchell S. Vascular malformations in the extremities: emphasis on MR imaging features that guide treatment options. *Skeletal Radiol* 2006; 35:127–137 [Erratum in *Skeletal Radiol* 2006; 35:964]
56. Kalmar JA, Salmon AP, Eick JJ, Merritt CR, Miller KD, Shuler SE. MRI of soft tissue vascular malformations. *J La State Med Soc* 1989; 141:27–32
57. Teh J, Whiteley G. MRI of soft tissue masses of the hand and wrist. *Br J Radiol* 2007; 80:47–63
58. Ohgiya Y, Hashimoto T, Gokan T, et al. Dynamic MRI for distinguishing high-flow from low-flow peripheral vascular malformations. *AJR* 2005; 185:1131–1137
59. Kern S, Niemeyer C, Darge K, Merz C, Laubenberger J, Uhl M. Differentiation of vascular birthmarks by MR imaging: an investigation of hemangiomas, venous and lymphatic malformations. *Acta Radiol* 2000; 41:453–457
60. Chhabra A, Soldatos T, Durand DJ, Carrino JA, McCarthy EF, Belzberg AJ. The role of magnetic resonance imaging in the diagnostic evaluation of malignant peripheral nerve sheath tumors. *Indian J Cancer* 2011; 48:328–334
61. Chhabra A, Thakkar RS, Gustav A, et al. Anatomic MR imaging and functional diffusion tensor imaging of peripheral nerve tumor and tumor like conditions. *AJNR* 2012(in press)
62. De Maeseneer M, Jaovisidha S, Lenchik L, et al. Fibrolipomatous hamartoma: MR imaging findings. *Skeletal Radiol* 1997; 26:155–160
63. Thawait SK, Chaudhry V, Thawait GK, et al. High-resolution MR neurography of diffuse peripheral nerve lesions. *AJNR* 2011; 32:1365–1372
64. Chhabra A, Faridian-Aragh N. High-resolution 3-T MR neurography of femoral neuropathy. *AJR* 2012; 198:3–10

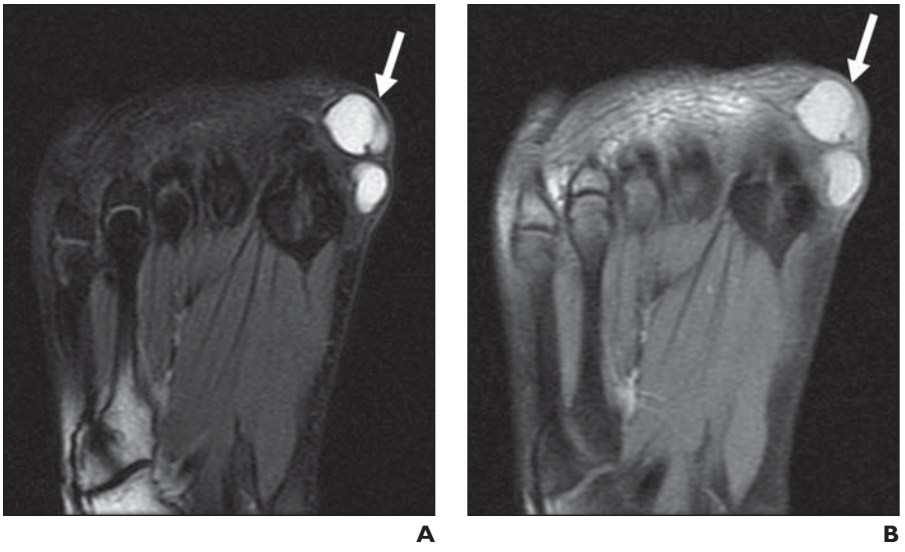

Fig. 1—24-year-old man with adventitial bursitis who presented with foot swelling and pain for few months. **A** and **B,** Coronal fat-suppressed T2-weighted (**A**) and unenhanced fat-suppressed T1-weighted (**B**) images of forefoot exhibit well-defined fluid collection (*arrow*) adjacent to first metatarsophalangeal joint. On unenhanced image (**B**), lesion is hyperintense, finding that should not be erroneously interpreted as contrast enhancement.

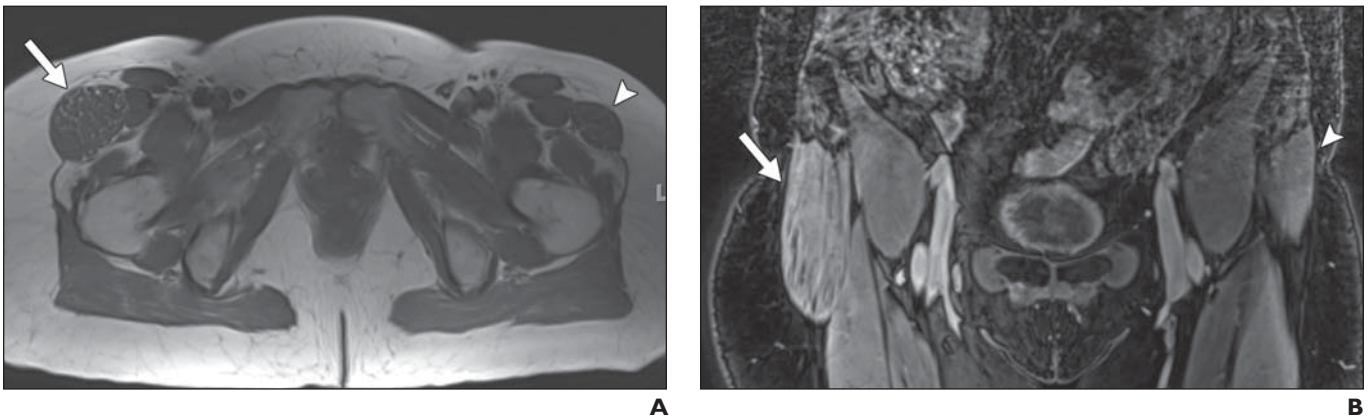

Fig. 2—51-year-old man with asymmetric muscle enlargement in pelvis.
A and **B,** Axial T1-weighted (**A**) and coronal fat-suppressed contrast-enhanced T1-weighted (**B**) images in patient with suspected soft-tissue sarcoma on outside imaging show asymmetric enlargement of right tensor fascia lata muscle (*arrow*) corresponding to palpable abnormality. Corresponding left-sided muscle (*arrowhead*) is normal in size.

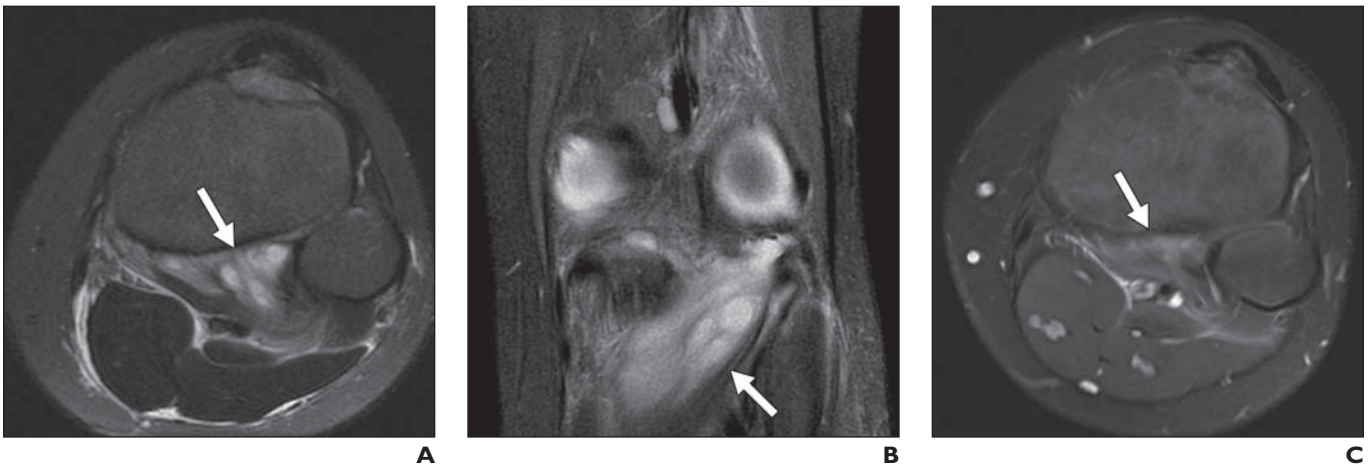

Fig. 3—15-year-old boy with muscle strain of left knee.
A and **B,** Axial (**A**) and coronal (**B**) fat-suppressed T2-weighted images show heterogeneous hyperintensity of popliteus muscle (*arrow*) attributed to asymmetric edema or hemorrhage.
C, Follow-up axial fat-suppressed T2-weighted image obtained 2 months after initial study shows partial resolution of muscle edema (*arrow*).

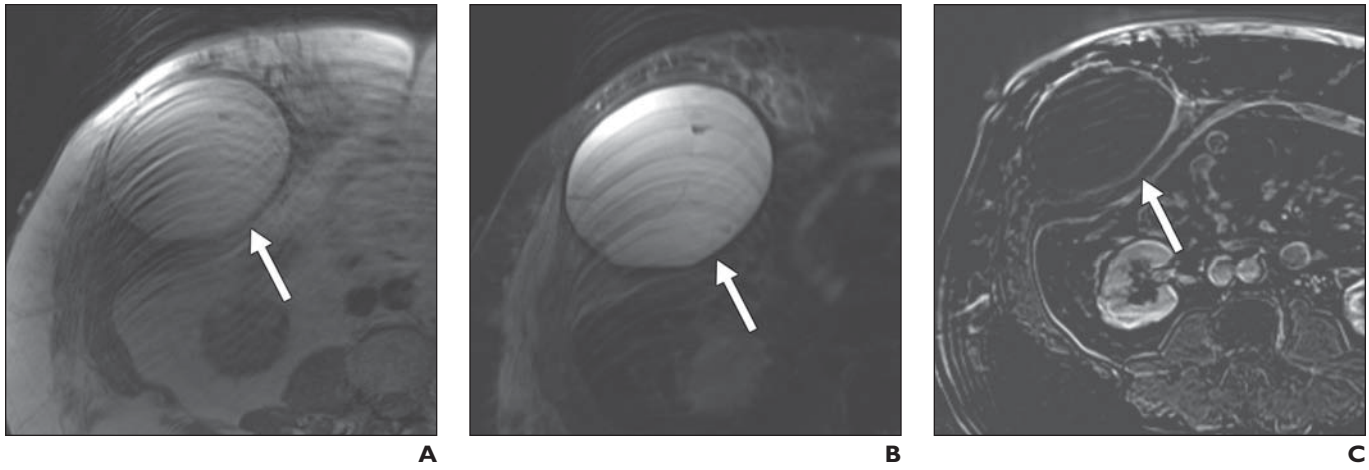

Fig. 4—45-year-old woman with subacute hematoma of anterior abdominal wall.
A–C, Axial T1-weighted (**A**), fat-suppressed T2-weighted (**B**), and fat-suppressed contrast-enhanced T1-weighted subtraction (**C**) images through abdomen show well-defined nonenhancing fluid collection (*arrow*) containing subacute blood.

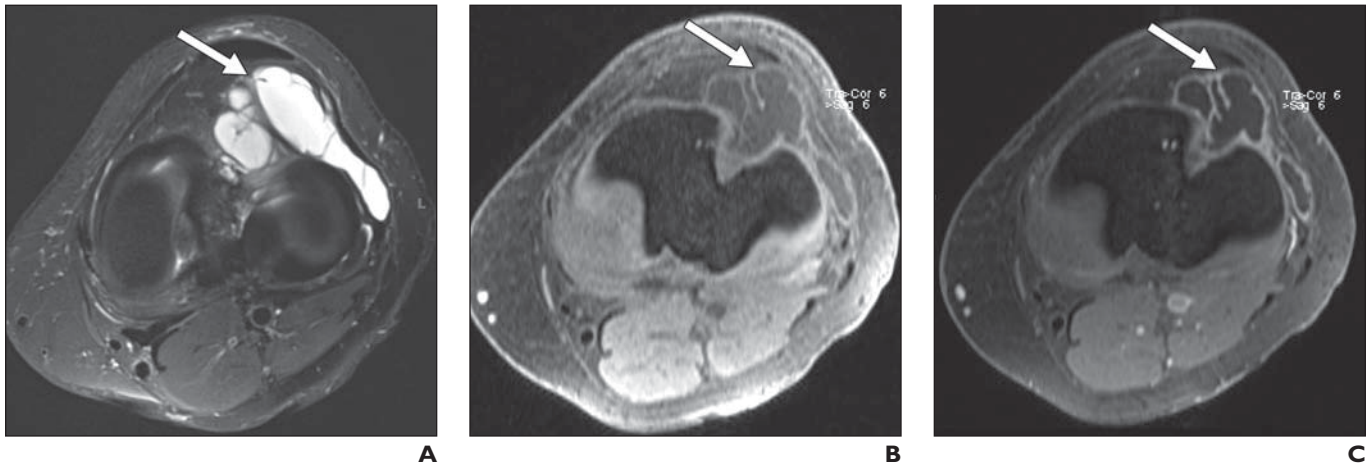

Fig. 5—42-year-old woman with ganglion cyst.
A–C, Axial fat-suppressed T2-weighted (**A**), unenhanced (**B**), and contrast-enhanced (**C**) fat-suppressed images through left knee show well-defined multilobulated fluid collection (*arrow*) with rim enhancement, consistent with ganglion cyst in relation to transverse ligament. Menisci were normal.

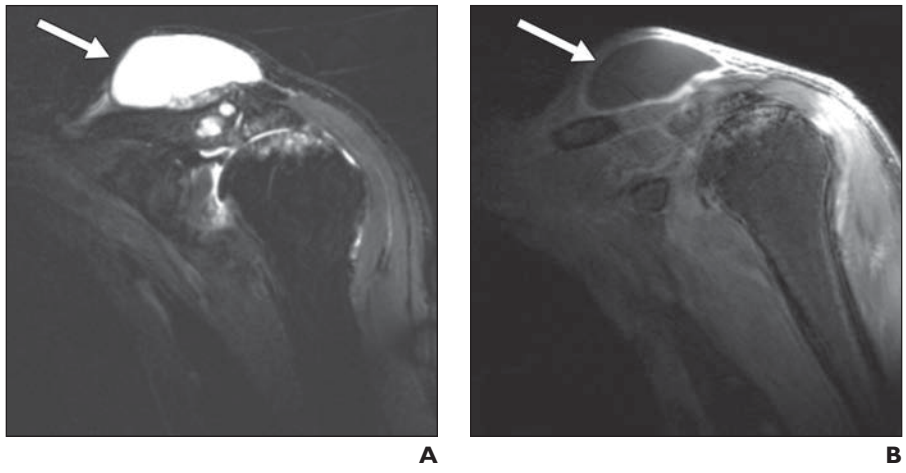

Fig. 6—61-year-old man with history of prostate carcinoma who presented with palpable mass at point of shoulder, which was found to be geyser phenomenon.
A and **B,** Sagittal fat-suppressed T2-weighted (**A**) and contrast-enhanced fat-suppressed T1-weighted (**B**) images through left shoulder show well-defined fluid collection (*arrow*) with rim enhancement, which lies in broad contact with acromioclavicular joint and projects in overlying subcutaneous tissues. Underlying chronic rotator cuff deficiency and arthropathy are present.

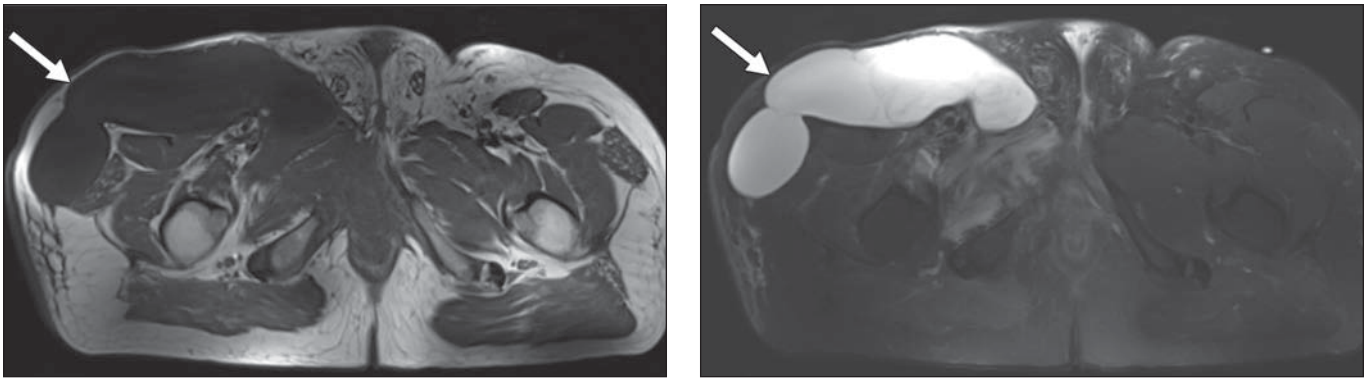

Fig. 7—43-year-old man with Morel-Lavallée lesion and remote history of pelvic injury.
A and **B,** Axial T1-weighted (**A**) and fat-suppressed T2-weighted (**B**) images through pelvic floor show well-defined multilobulated fluid collection (*arrow*) located between skin and underlying fascia. Lesion regressed over period of few months.

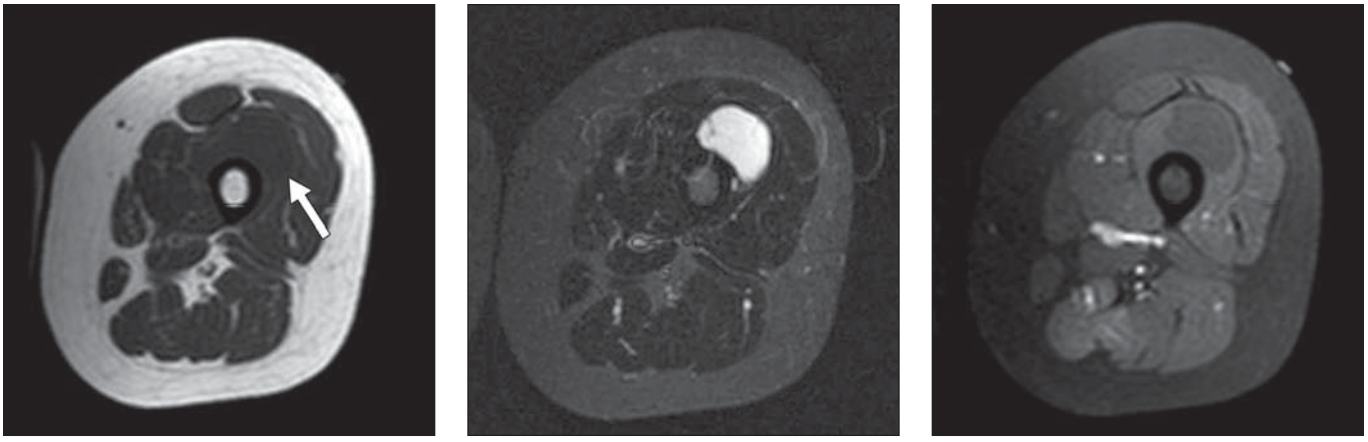

Fig. 8—53-year-old woman who presented with mild thigh pain due to cystic myxoma.
A–C, Axial T1-weighted (**A**), STIR (**B**), and fat-suppressed contrast-enhanced T1-weighted (**C**) images through midthigh show peripherally enhancing cystic lesion (*arrow*, **A**), which was biopsy proven to be benign myxoma.

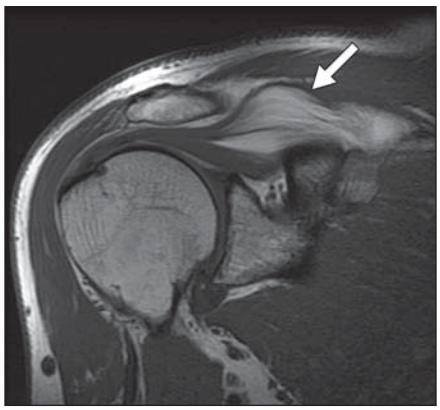

Fig. 9—65-year-old man with intramuscular lipoma.
Coronal T1-weighted image of right shoulder shows space-occupying lesion (*arrow*) with signal analogous to fat, within supraspinatus muscle.

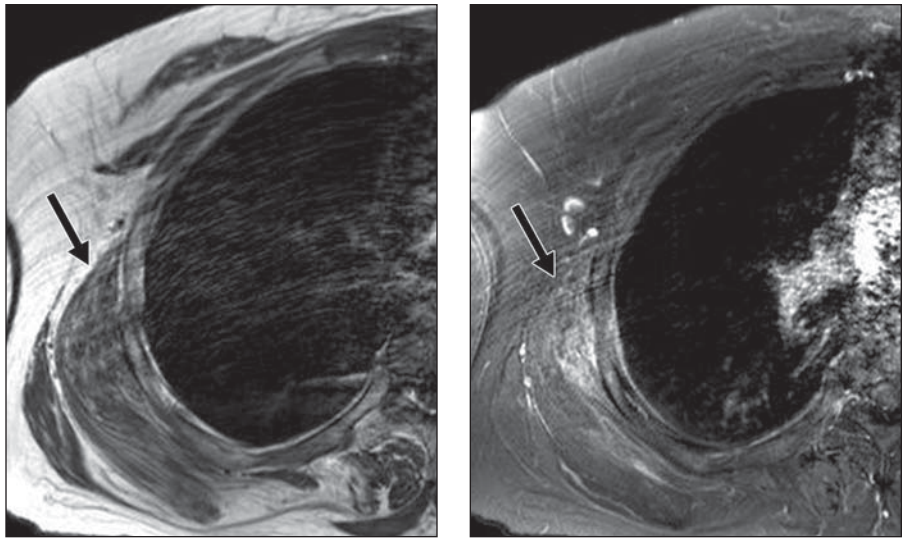

Fig. 10—56-year-old woman with elastofibroma dorsi manifesting as palpable mass in right axilla.
A and **B,** Axial T1-weighted (**A**) and fat-suppressed T2-weighted (**B**) images through upper thorax show space-occupying lesion (*arrow*) between inferomedial border of scapula and latissimus dorsi muscle, featuring fibrofatty striations, classic appearance, and location of elastofibroma dorsi.

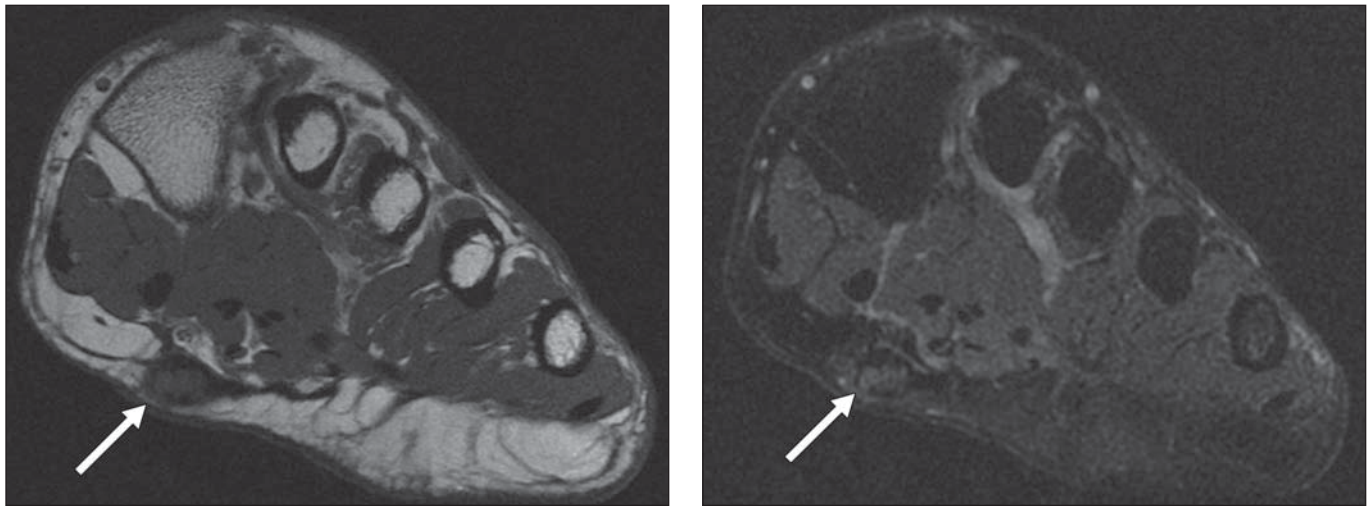

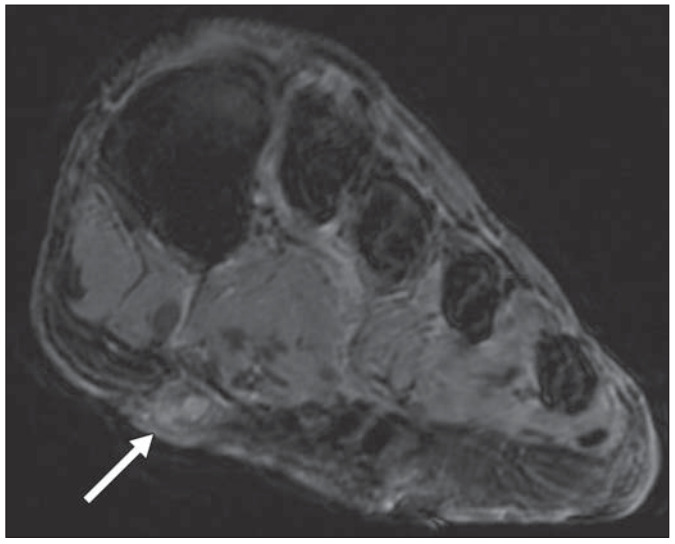

Fig. 11—40-year-old man with plantar fibroma.
A–C, Axial T1-weighted (**A**), fat-suppressed T2-weighted (**B**), and fat-suppressed contrast-enhanced T1-weighted (**C**) images of midfoot show enhancing pea-shaped lesion (*arrow*) in relation to central cord of plantar fascia, consistent with fibroma.

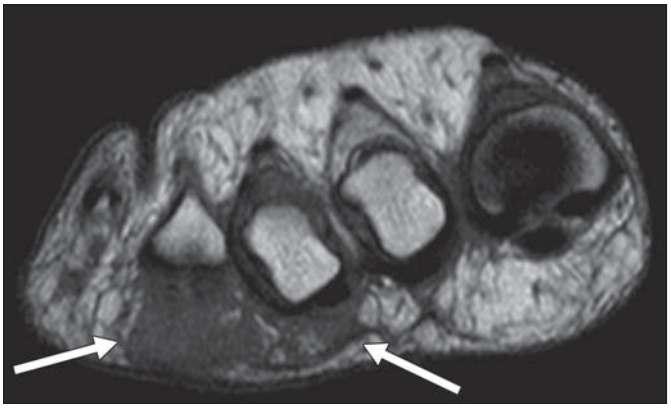

A

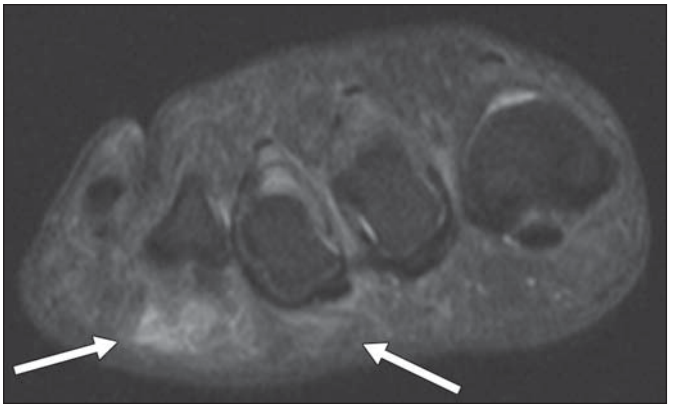

B

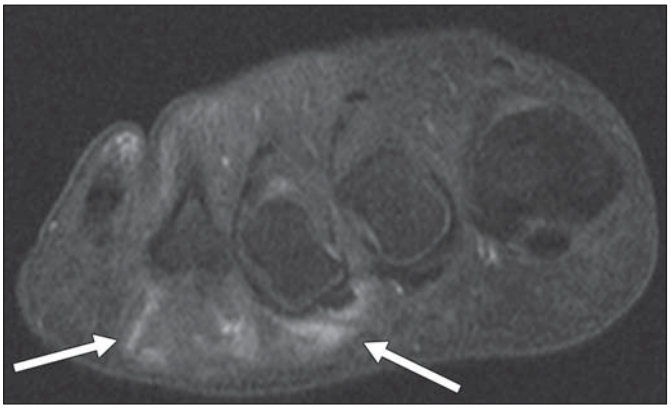

C

Fig. 12—45-year-old woman with plantar callous who presented with pain and swelling for 6 months along ball of third and fourth toes, worsening in last 2 weeks. **A–C,** Axial T1-weighted (**A**), fat-suppressed T2-weighted (**B**), and fat-suppressed contrast-enhanced T1-weighted (**C**) images of forefoot show T1-isointense predominantly T2-hypointense space-occupying lesion (*arrows*) underneath third and fourth metatarsals with poor enhancement, consistent with callous formation.

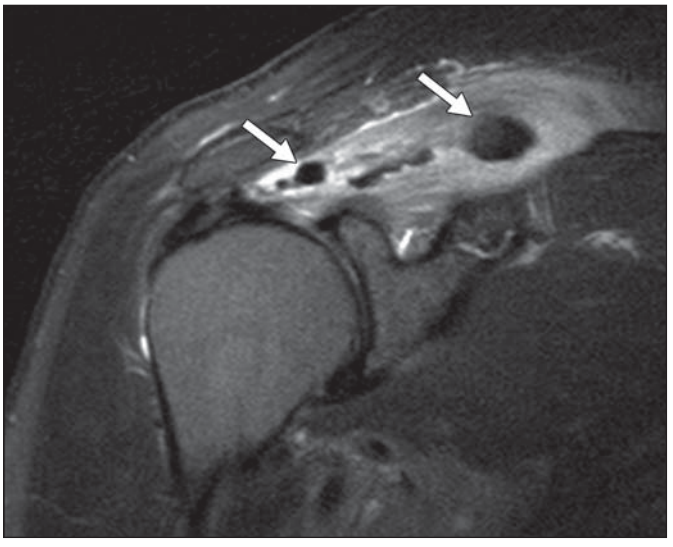

Fig. 13—56-year-old man with hemosiderin deposition and hydroxyapatite deposition disease. Coronal fat-suppressed T2-weighted image of right shoulder shows extensive edema and inflammation of supraspinatus muscle with multiple hypointensities (*arrows*) in muscle belly consistent with hemosiderin deposition and hydroxyapatite deposition disease.

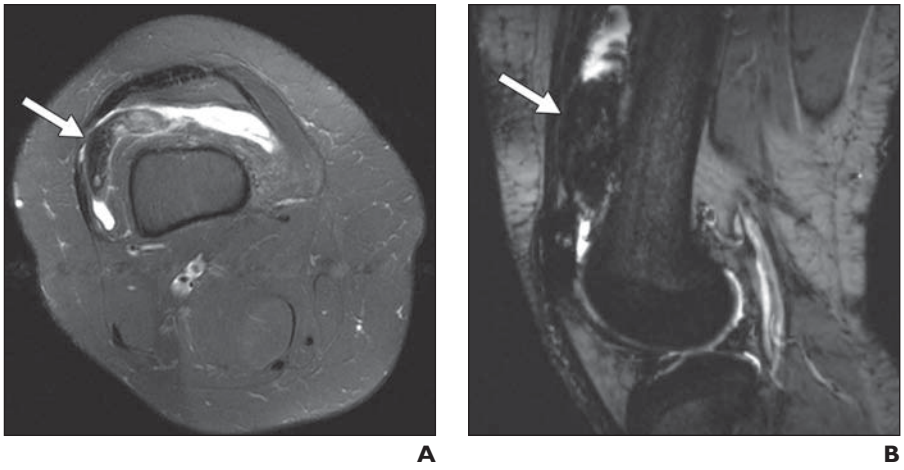

Fig. 14—35-year-old man with pigmented villonodular synovitis.
A and **B,** Fat-suppressed axial T2-weighted (**A**) and sagittal T2*-weighted (**B**) images of right knee show hypertrophied synovium (*arrow*), presenting as focal masslike lesion of low signal intensity. Notice blooming on T2*-weighted image.

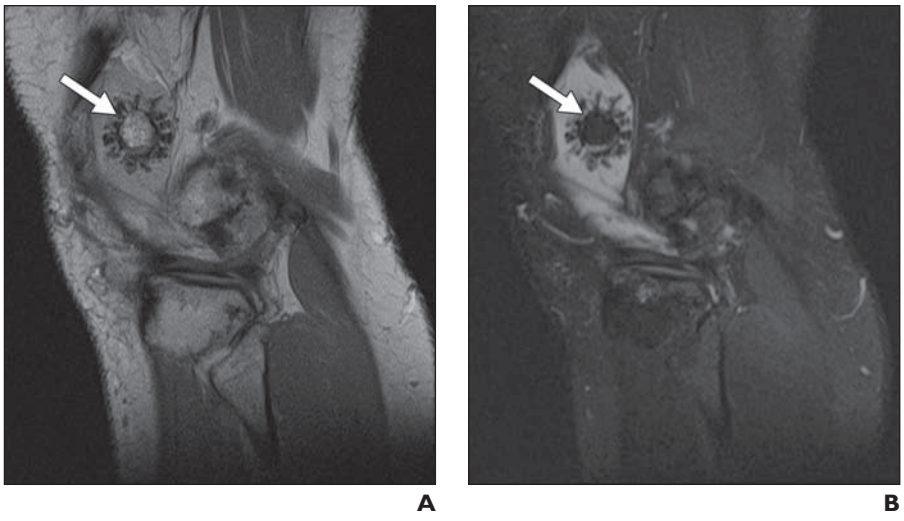

Fig. 15—46-year-old woman with loose osteochondral body.
A and **B,** Sagittal proton density–weighted (**A**) and fat-suppressed T2-weighted (**B**) images of knee show loose osteochondral body (*arrow*) containing central marrow signal within lateral aspect of suprapatellar bursa.

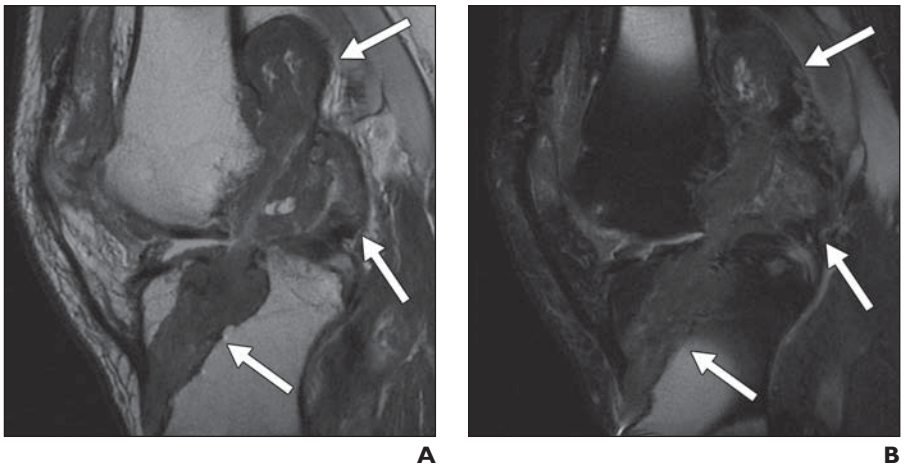

Fig. 16—69-year-old man with previous failed anterior cruciate ligament reconstruction.
A and **B,** Sagittal T1-weighted (**A**) and fat-suppressed T2-weighted (**B**) images of knee show extensive soft tissue (*arrows*) occupying femoral and tibial tunnels. Findings are consistent with particle disease.

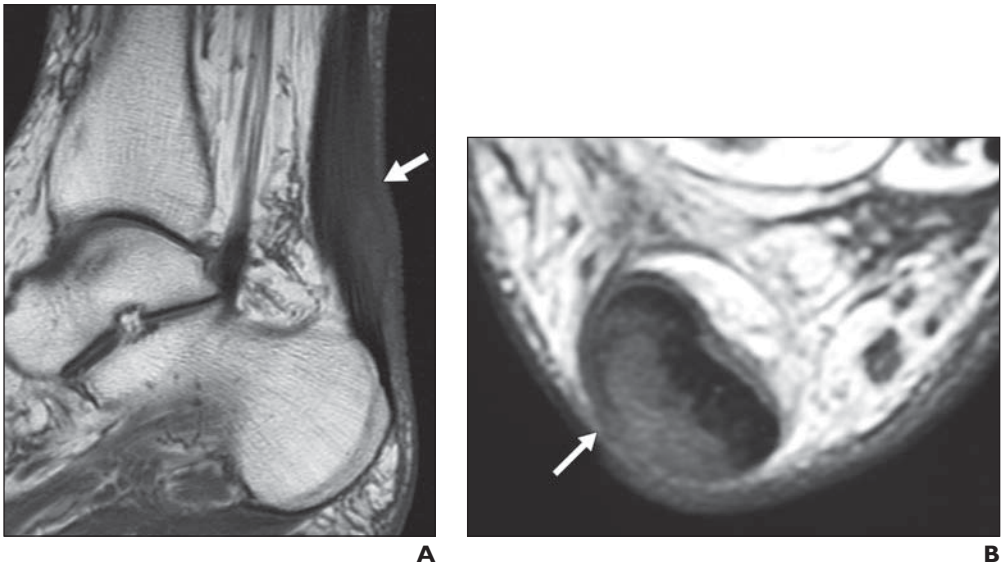

Fig. 17—45-year-old man with intratendinous xanthoma and hypercholesterolemia.
A and **B,** Sagittal T1-weighted (**A**) and axial T2-weighted (**B**) images of hindfoot exhibit focal enlargement (*arrow*) of Achilles tendon, featuring reticulated architecture and heterogeneous signal intensity.

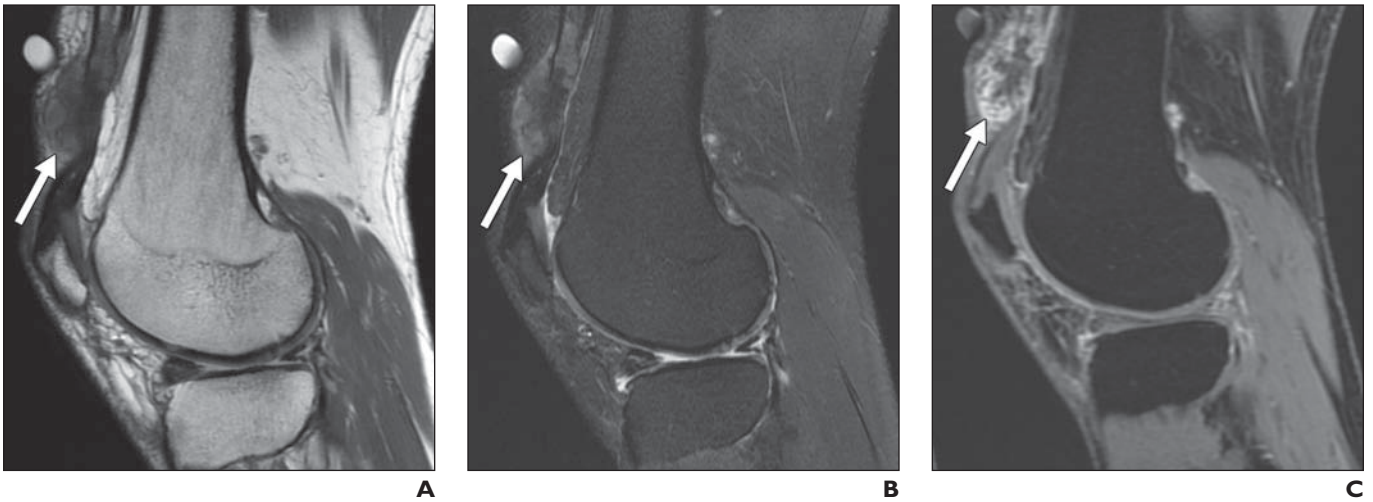

Fig. 18—41-year-old man with intratendinous gout.
A–C, Sagittal proton density–weighted (**A**), fat-suppressed T2-weighted (**B**), and fat-suppressed contrast-enhanced T1-weighted (**C**) images of knee show focal hypointense and peripherally enhancing lesion (*arrow*) in quadratus tendon. Patient had known increased uric acid levels. Biopsy was also positive for gout deposit.

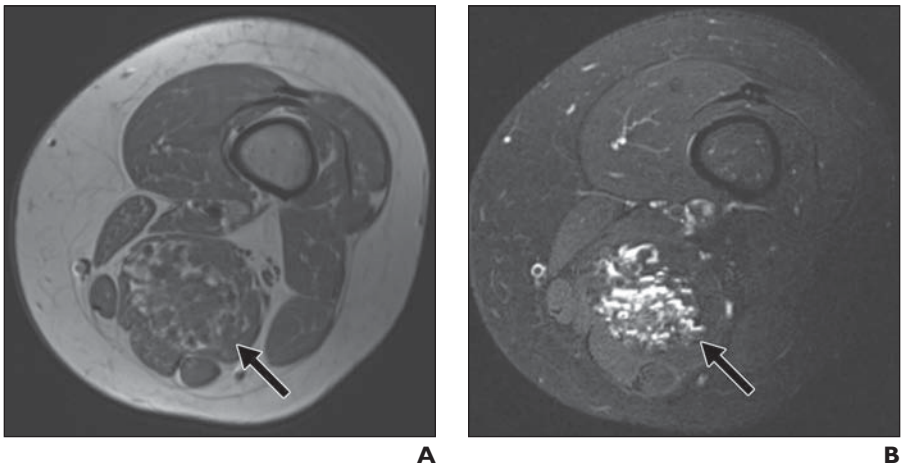

Fig. 19—36-year-old woman with intramuscular venous malformation.
A and **B,** Axial T1-weighted (**A**) and fat-suppressed T2-weighted (**B**) images through lower femur show heterogeneous lobulated space-occupying mass (*arrow*) featuring wormlike vascular channels, with fluid levels in semimembranous muscle.

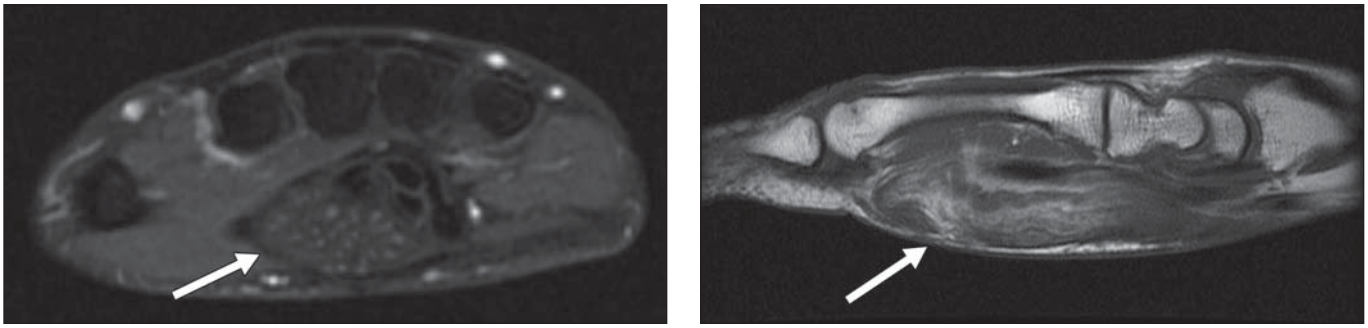

Fig. 20—54-year-old man with fibrolipomatous hamartoma of median nerve.
A and **B,** Axial fat-suppressed T2-weighted (**A**) and sagittal T1-weighted (**B**) images of hand show focal fusiform enlargement of median nerve (*arrow*), associated with fatty proliferation and thickening of nerve bundles. Notice coaxial cable appearance of median nerve in axial image and spaghetti appearance in long-axis image.

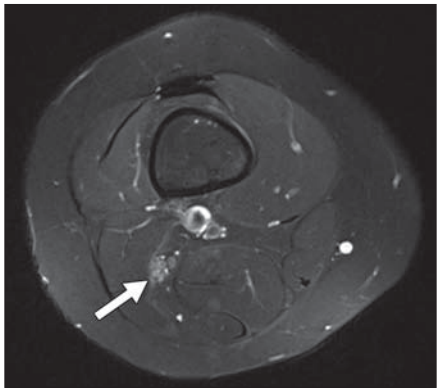

Fig. 21—15-year-old girl with perineurioma of sciatic nerve. Axial fat-suppressed T2-weighted image through femur shows honeycomblike fascicular enlargement of sciatic nerve (*arrow*) in this biopsy-proven case.